Microgravity Sci. Technol. (2017) 29:229–239
DOI 10.1007/s12217-017-9542-0

ORIGINAL ARTICLE

Electrically Charged Droplets in Microgravity

Impact and Trajectories

Martin Brandenbourger[1] · Hervé Caps[1] · Youen Vitry[2] · Stéphane Dorbolo[1]

Received: 25 November 2016 / Accepted: 26 February 2017 / Published online: 13 March 2017

Abstract In this work, the interaction between electrically charged droplets in microgravity is considered. During the 22 s of microgravity brought by a parabolic flight, water droplets with a radius $r \in [0.41 - 0.97]$ mm were released one in front of the other. A high-speed camera allowed studying their interaction in the focal plane. The trajectories of the droplets are well adjusted by a punctual charge model. In some experiments, a physical contact between the charged droplets was observed. These collisions are studied via a phase diagram comparing the droplet Weber number, We, and the collision parameter, χ. By comparing these collisions to experiments involving neutral droplets, we deduce how the collision diagram is affected by electric charges. In particular, we show that the criterion for an impact between two droplets is no more $\chi < 1$.

Keywords Charged drop · Thunderclouds · Electric interaction · Collision diagram · Impact

Introduction

The physics of collisions between droplets has raised the interest of several scientists since the early 1950s (Swinbank 1947; Davis and Sartor 1967; Brazier-Smith et al. 1972). In the particular case of water droplets, this interest comes specifically from atmospheric research (Testik 2009; Beard et al. 2001; Franklin et al. 2005). The experiments were focused on small droplets (i.e. $r \approx 150$ μm to represent cloud droplets) and large drops (i.e. $r \approx 1$ mm to represent raindrops). The main goal of these studies was to understand how several collisions between droplets could affect their radius distributions. Indeed, when droplets collide, they can bounce on each other, stick together or separate in several smaller droplets. Previous studies investigated which parameters affect the droplet impact. For example, Ashgriz and Poo (1990) have shown that impact between drops depends on their respective radius, speed and angle of impact. Furthermore, Qian and Law (1997) showed that the result of the impact also depends on the ambient air pressure and the liquid composition.

In the literature (Ashgriz and Poo 1990; Qian and Law 1997; Gotaas et al. 2007), the collision between two neutral droplets (a and b) of the same volume (i.e. the same radius, $r_a = r_b = r$) and composition is commonly described by a phase diagram comparing the collision parameter χ with the Weber number We. These parameters are respectively defined by:

$$\chi = \frac{x}{(r_a + r_b)} \tag{1}$$

$$We = \frac{\rho v_{rel}^2 (r_a + r_b)}{\gamma} \tag{2}$$

where x is the projected separation distance between the centers of the colliding droplets normal to the relative velocity vector $\vec{v}_{rel}$ (see Fig. 1), r_a and r_b are the radii of each

Electronic supplementary material The online version of this article (doi:10.1007/s12217-017-9542-0) contains supplementary material, which is available to authorized users.

✉ Martin Brandenbourger
martinbdbg@gmail.com

[1] CESAM-GRASP, Physics Department, University of Liège, B-4000, Liège, Belgium

[2] TIPs, Université Libre de Bruxelles, Bruxelles, Belgium

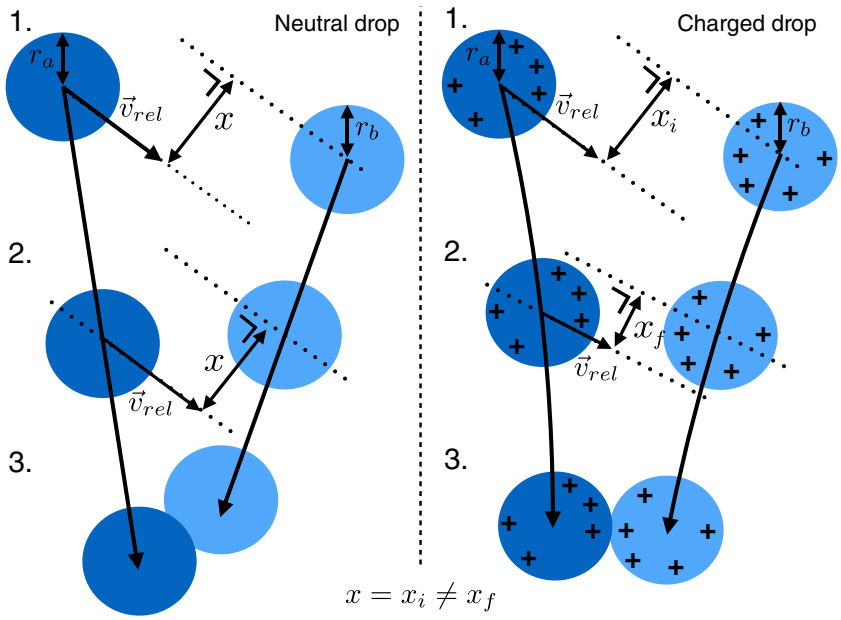

Fig. 1 (Color online) Schema of the relative droplet motion for neutral (*left*) and charged droplets (*right*). Neutral droplets move straight on, while the trajectory of charged droplets is affected by their electric interaction. The relative speed between both droplets corresponds to the vector $\vec{v}_{rel}$. While the distance x remains constant for neutral droplets, it varies over time for charged droplets because of the electric interaction. The collision parameter χ is calculated from the distance $x = x_i$ and the radii r_a and r_b

droplet, ρ is the droplets density and γ is the droplets surface tension. In the case of neutral droplets, two droplets sent toward each other are generally supposed to move straight until impacting. As a consequence, the direction of the relative speed v_{rel} does not vary over time, which means that the collision parameter is also constant over time.

According to the parameters χ and We, the collision between neutral droplets leads to different behaviors. The collision diagram, shown in Fig. 2, points out each of these behaviors. If $\chi > 1$, the droplets do not contact each other. If $\chi < 1$, both droplets impact each other. Four different impacts can be observed: the bouncing between droplet, the coalescence, the stretching separation and the reflexive separation (examples of collisions are accessible in Supplemental Materials). The frontiers between each impact behavior on the collision diagram were previously studied experimentally and theoretically. Figure 2 was built from the results obtained by Ashgriz and Poo (1990) and Gotaas et al. (2007) with water at ambient pressure.

Studies such as Ashgriz and Poo (1990) and Qian and Law (1997) led to a better understanding of the collision between two neutral droplets. However, in the case of droplets with an excess of electric charges, the system acquires one more degree of freedom. Indeed, the electric attraction or repulsion between droplets adds an interaction, which influences the collision before and during the impact between droplets. A natural example of the differences existing between the collisions of neutral or charged droplets is the contrast between clouds and thunderclouds (Leblanc et al. 2008).

In order to study the interaction between charged droplets, various approaches have been implemented. Studies have been specifically focused on the simulation of several charged droplets interacting with each other (Khain et al. 2004) while others have been focused on direct measurements (Beard et al. 2002; Beard et al. 2001; Snarski and Dunn 1991; Abbott 1974). These measurements always involve one droplet falling on another because of gravity

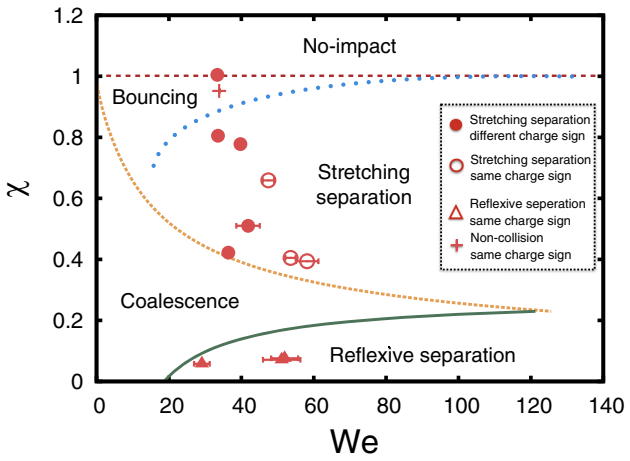

Fig. 2 (Color online) Collision diagram for charged droplets (*symbols*) as compared to theoretical predictions for neutral droplets (*lines*). The y-axis corresponds to the collision parameter χ (Eq. 1). The x-axis corresponds to the Weber number *We* (Eq. 2). The *orange dashed line* describes the theoretical frontier between coalescence and stretching. *The green line* describes the theoretical frontier between coalescence and reflexive separation. Both theoretical predictions come from Ashgriz and Poo (1990). The *blue points* describe the frontier between stretching and bouncing between droplets (deduced from measurements of Gotaas et al. (2007). The *red circles*, triangles and crosses describe the observed collisions between charged droplets. The *red cross* corresponds to an experiment performed with the same sign of charges. The error bars account for the small difference in radii between both colliding droplets. Examples of collisions are accessible in (Supplemental Materials)

or several droplets (two charged jets) interacting with each other. They showed that the electric interaction between two droplets could be modeled as the interaction between two charged conducting spheres (Khain et al. 2004).

Even if studies investigated the collision between two charged droplets (Beard et al. 2001, 2002; Abbott 1974, there is, to our knowledge, no comparison between the collision diagram of neutral droplets and the collision between charged droplets. This lack of results is explained by the difficulty to highlight the influence of the electric interaction on the droplet trajectories. Indeed, a rapid calculation of the electric force between two charged droplets shows that the electric force is 40 times smaller than the droplet weight. As a consequence, two charged droplets sent toward each other mainly endure the acceleration of gravity. They quickly acquire an important speed and the electric interaction becomes negligible compared to aerodynamic interactions. Therefore, studies did not observe an influence of the electric charges (Adam et al. 1968) on the droplets collisions or were limited to collision parameters $\chi \approx 0$ (Beard et al. 2002; Beard et al. 2001; Abbott 1974).

Therefore, a precise understanding of the impact between droplets as a function of the collision parameter χ and the Weber number We is still needed. Indeed, in systems made of several droplets colliding with each other, the impact between droplet can occur on a wide range of collision parameter χ and weber number We. In order to track the result of these numerous collisions, we need to understand what is the influence of the electric charges on each kind of collisions. Moreover, the electric interaction also influences the possibility of an impact between droplets. A better knowledge on the collision diagram of charged droplets would allow to better predict the evolution of systems such as thunderclouds (Khain et al. 2004). Furthermore, new applications based on the collision of droplets, such as spreading techniques (Damak et al. 2016) or 3D printing (Visser et al. 2016) would benefit greatly from this information. Indeed, the Weber number of the ejected droplet could be adjusted in order to promote specific impacts between drops.

In the following Sections, we propose to compare collisions between charged droplets to collisions between neutral droplets on a large range of We and χ. In order to maximize the influence of the electric charges, we focused our study on the interaction between two electrically charged droplets with a radius $r \in [0.41-0.97]$ mm interacting in microgravity conditions. The specific range of radius was chosen to maximize the influence of the electric charge. Indeed, while the charge of micrometric droplets is about 0.01 pC (Khain et al. 2004), our charged droplets had charges of about 100 pC. As shown in previous studies, the microgravity is a good tool to study the interaction between droplets and electric charges (Imamura et al. 2005).

A typical experiment is shown in Fig. 3. For clarity, this experiment corresponds to droplets that do not impact with each other. On each side of the image, a charged droplet generator ejects a droplet. Images separated by 4 ms have been superposed in order to visualize the droplets motion. Because of the microgravity conditions, the droplets move in the direction indicated by their initial speed. Once they come closer to each other, their displacement is influenced by their electric interaction.

Experimental Setup

In the next lines, we describe how the microgravity condition was reached and the diverse setups that were developed in order to perform the experiments.

The microgravity condition was obtained thanks to ESA parabolic flights performed by Novespace http://www.novespace.fr/. During such flights, the airplane performed portions of a parabola. At the top of the parabola, the lift and the drag compensate and the effect of gravity is reduced to almost zero. Over all the parabola, we measured a maximum deviation from microgravity conditions equal to 0.05 g, with g being the earth gravity. The results presented in the article have been obtained in a period of three days, which corresponds to 93 parabolas. Each parabola corresponds to 22 s of microgravity. Several experiments are run on each parabola, in which two electrically charged droplets are shot against each other. A typical experiment is presented by the image superposition in Fig. 3.

To generate electrically charged droplets in microgravity, a specific apparatus was built. The apparatus is shown in Fig. 4 (top), which depicts two charged-droplet ejectors facing each other. A detailed schema of one charged droplet

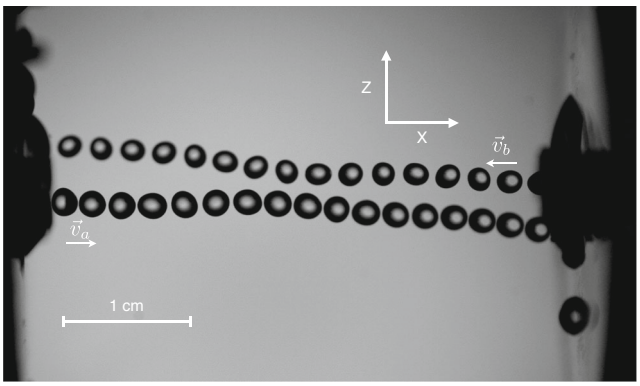

Fig. 3 Image superposition of a typical experiment. Two droplets were sent toward each other thanks to two charged droplet generators. The droplet initial speeds correspond respectively to $\vec{v}_a$ and $\vec{v}_b$. Four milliseconds separate each droplet. We observe that the droplet motion is affected by the electric interaction between droplets. The focus plane of the high-speed camera is called XZ

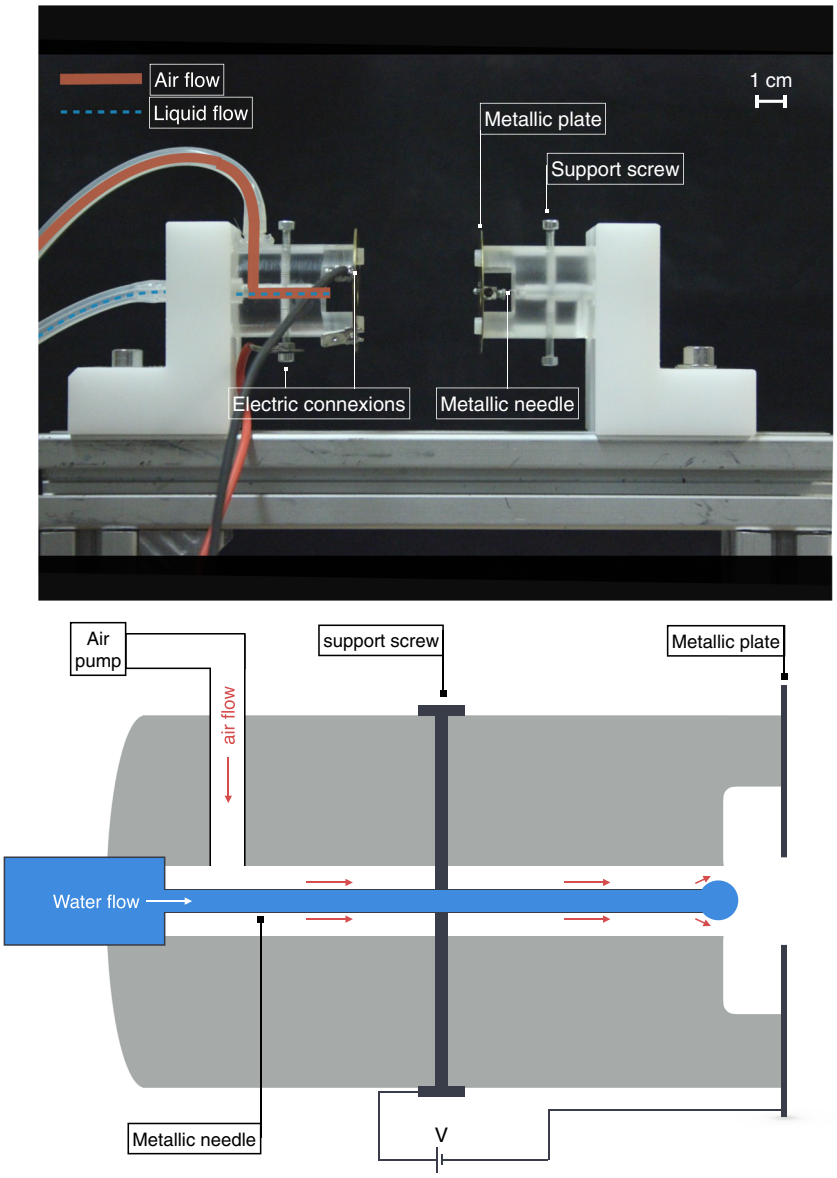

Fig. 4 (Color online) (*top*) Picture of two charged droplet generators facing each other. (*bottom*) Schema of the charged droplet generator. A voltage is set between the metallic needle and the metallic plate, generating charge migration. The droplets are then ejected thanks to coaxial airflows

generator is shown in Fig. 4 (bottom). A cylindrical plastic piece (in grey) encircled a metallic needle. A metallic plate was fixed at the edge of the plastic piece. A hole in the plastic piece allowed air to flow around the needle. Two support screws were screwed up in the plastic piece in order to maintain the metallic needle location. A voltage generator allowed controlling the voltage between the support screw (connected to the metallic needle) and the metallic plate. The charged droplet generator was coupled to an air pump. As shown in Fig. 4, laminar airflow was generated around the needle. In order to generate a charged droplet, we firstly accumulated liquid at the edge of the metallic needle. This was done by controlling the water flow injected in the metallic needle. Then, the airflow detached and blew away the charged droplet. By controlling the airflow, it was possible to control the droplet generation rate and the droplet size.

The charging of the droplets was performed via charges migration due to an external electric field. A voltage difference was applied between the metallic plate and the metallic needle in order to generate an electric field. When a droplet was at the edge of the needle, electric charges migrated from the liquid contained in the needle to the droplet. As the droplet leaves the needle, it carried on an excess of electric charges. The number of electric charges induced in the droplet is linked to the scalar value of the electric field at the edge of the needle. As a consequence, the charge only depends on the generator geometry, the droplet surface and the voltage between the metallic plate and the needle (see, for example, Brandenbourger and Dorbolo 2014).

Parabolas have been dedicated to the droplet charge measurement. The charge measurement was performed thanks to a Faraday cup and an electrometer (Keithley 6514). These

measurements allowed calibrating the charged droplet generator. From this calibration, the charge of the droplet was deduced for any radius of an electrically charged droplet.

The motion of the droplets was recorded at 2000 fps using a high-speed camera (Phantom MIRO M310). The image superposition in Fig. 3 shows the droplet motion recorded in the XZ plane. For all the experiments, the distance between both metallic plates was kept equal to 41 mm.

Droplet Trajectories

In this Section, we first investigate the experiments that did not lead to impact between droplets. For neutral droplets, the non-collision corresponds to $\chi > 1$ on the collision diagram (see Fig. 2). Naturally, the frontier between collision and non-collision can eventually be changed by the electric interaction. As shown in Fig. 3, because of electric interactions, droplets do not move in a straight line. The goal of the present Section is to describe the specific trajectories of these droplets as a function of their relative electric interaction. Such a description allows deducing assumptions on electric interactions between droplets during events that lead to a collision.

Results

Figure 5 shows two examples of experiments performed in microgravity. The graphs on the left side (A. and C.) show the relative horizontal ($\Delta x = x_a - x_b$) and vertical ($\Delta z = z_a - z_b$) droplet positions over time of two electrically charged droplets in the XZ plane. The charges and the radii of each droplet is indicated in Table 1. The first experiment (A.) corresponds to charged droplets with the same sign of charge (Table 1, case +/+). The curvature of the trajectories changes when the droplets are near each other ($\Delta x \approx 0$), meaning that the droplets influence each other. The second graph on the left (C.) corresponds to two droplets with opposite charges (Table 1, case +/-).

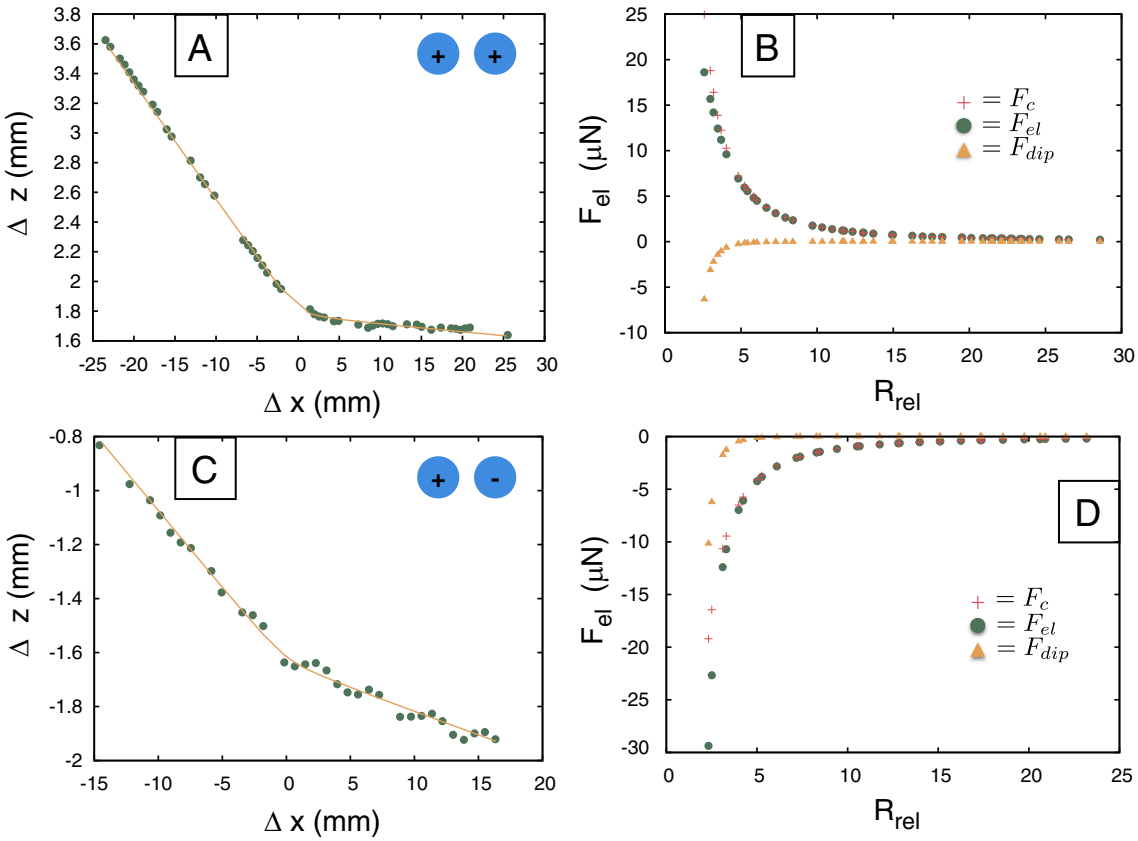

Fig. 5 (Color online) The graphs **A.** and **B.** show an experiment performed with droplets of the same sign of charge, corresponding to the case +/+ in Table 1. The graphs **C.** and **D.** show an experiment performed with droplets of opposite signs of charges, corresponding to the case +/- in Table 1. The graphs on the *left side* describe the relative position Δx and Δz of two droplets during their motion in the plane XZ. The orange curves correspond to fits of the trajectory taking into account a Coulomb interaction (see Eq. 7). The graphs on the *right side* compare the value of the Coulomb force (*red crosses*), the dipole force (*orange triangles*) and the total electric force (*green points*) as a function of the relative position R_{rel}

Table 1 Characteristics of both experiments described in Fig. 5

	Case +/+	Case +/-
$q_a(pC)$	−56.6	−91.3
$q_b(pC)$	−56.6	63.2
r_a (mm)	0.86	0.77
r_b (mm)	0.97	0.64
v_{rel} (m/s)	1.08	1.64
p_{theo}	0.3206	0.0821
p_{fit}	0.3386	0.0824
$p_{err}(\%)$	5.3	0.4
e_{theo}	146.1838	48.9406
e_{fit}	156.9317	50.0385
$e_{err}(\%)$	6.84	2.2

The symbols $q_{a/b}$ and $r_{a/b}$ correspond respectively to the charge and the radius of each droplet. The relative initial speed between two droplets is indicated by the symbol v_{rel}. The symbols $p_{theo/fit}$ and $e_{theo/fit}$ correspond to the two parameters from Eq. 7 respectively deduced from the droplet parameters or the droplet trajectories. Finally, p_{err} and e_{err} indicate the relative error between each of the two previous parameters

Contrarily to the previous cases, we observe that the relative distance between droplets increases less quickly after their crossing. In other words, the curvature of the function is inverted, indicating an attraction between droplets.

The graphs on the right side of the Fig. 5B and D show the calculated electrical force between the droplets as a function of their relative position $R_{rel} = 2r/(r_a + r_b)$, where r is the distance between the center of mass of the droplets and r_a and r_b are the droplet radii. The considered electric force takes into account the monopole-monopole, monopole-dipole and dipole-dipole interactions:

$$\begin{aligned} F_{el} &= F_c + F_{dip} \\ &= \frac{q_a q_b}{4\pi\epsilon_0 r^2} + \frac{1}{4\pi\epsilon_0} q_a^2 r_b \left(\frac{1}{r^3} - \frac{r}{(r^2 - r_b^2)^2} \right) \\ &+ \frac{1}{4\pi\epsilon_0} q_b^2 r_a \left(\frac{1}{r^3} - \frac{r}{(r^2 - r_a^2)^2} \right) \\ &+ \frac{1}{4\pi\epsilon_0} q_a q_b r_a r_b \left(\frac{1}{r^4} + \frac{1}{(r^2 - r_a^2 - r_b^2)^2} \right. \\ &\left. - \frac{1}{(r^2 - r_a^2)^2} - \frac{1}{(r^2 - r_b^2)^2} \right) \end{aligned} \tag{3}$$

where $F_c = \frac{q_a q_b}{4\pi\epsilon_0 r^2}$ corresponds to the Coulomb interaction and the rest of the equation, F_{dip}, corresponds to the dipolar forces. The charges q_a and q_b are respectively the electric charges of droplets a and b and ϵ_0 corresponds to the vacuum electrical permittivity.

As expected, the first case described in Fig. 5B corresponds to repulsive forces while the second case (D.) corresponds to attractive forces between droplets. The curves also show that, in most of the cases, the dipolar component of the electric force is mainly negligible until a distance between droplets corresponding to approximately 3 R_{rel}. Indeed, the green points and the red crosses are superposed during the majority of the experiments. Beyond these two examples, it as to be noted that we observed the same behavior over more than ten analyzed droplet trajectories.

Discussion

As stated in the previous section, we were able to observe several charged droplet trajectories. The observations showed that the electric interactions between droplets influence their trajectories. In the next lines, we aim at describing quantitatively these trajectories.

In order to understand the trajectories of each droplet, we need to consider the electric force F_e (see Eq. 3) describing the Coulomb and dipolar interactions which influence both droplet. While the Coulomb interaction describes only the interaction between static charges, the dipolar force takes into account the motion of the electric charges inside the droplet. As a consequence, taking into account the dipolar interaction means that the time for a charge to move in the droplet is considered negligible with respect to the time scale of the droplet motion. In order to check the validity of this assumption, we estimate the characteristic time scale of the charge displacement as (for more details, see Pfeifer and Hendricks 1967):

$$\tau = \epsilon_r \epsilon_0 / \sigma \tag{4}$$

where ϵ_r and σ are respectively the relative permittivity and the conductivity of the liquid. In the case of bidistillated water, $\tau = 0.13$ ms. Figure 5 shows that the interaction between both electrically charged droplets becomes non-negligible at a distance of approximately 3 mm ($r < 3R_{rel}$). If we take a droplet speed of $v = 1$ m/s (which is in accord with Table 1), it takes 3 ms for a droplet to travel this distance. We deduce that the timescale of the charge displacement is negligible compared to the motion time scale of both electrically charged droplets. However, the small distance at which dipole interaction becomes non-negligible ($r < 3R_{rel}$) indicates that the dipole interaction should have a small influence on the droplets motion. As a consequence, the first step is to describe each droplet trajectory by only taking into account the Coulomb force. Note that the dipolar interaction could eventually be non-negligible in systems involving higher electric charges and smaller drop radii. With this assumption, the droplet trajectory can be seen as a two-body problem influenced by a Newtonian force:

$$\vec{F}_N = \frac{k}{r^2} \vec{u}_r \tag{5}$$

where k is a constant (in our case $k = q_a q_b / 4\pi\epsilon_0$), r is the relative distance between the droplets and u_r is a unit

vector. The classical way to resolve this two-body system is to reduce the problem to a one-body system influenced by a central force:

$$\mu \frac{d^2\vec{r}}{dt^2} = \vec{F}_N \tag{6}$$

The reduced mass is $\mu = \frac{m_a m_b}{m_a + m_b}$, where m_a and m_b correspond respectively to the mass of the droplet a and b. This classical problem has a solution in polar coordinates (r, θ). From Eq. 6 the distance between the charged droplets as a function of θ is expressed as:

$$r(\theta) = \frac{p}{(\mp)1 + e\cos(\theta - \theta_0)} \tag{7}$$

where $p = \frac{(\pm)\mu C^2}{k}$ and $e = (\pm)(\frac{p}{r_0} + 1)$. The sign $(\pm)$ corresponds respectively to droplets with the same sign of charges or with different signs of charges. The constant $C = r^2\dot{\theta}$ is derived from the angular momentum conservation and r_0 is the minimal distance between droplets.

The trajectories on the Fig. 5 have been adjusted by Eq. 7. The results of the fits correspond to the orange lines on the Fig. 5A and C. A comparison between the fitting parameters and the measured value of p_{theo} and e_{theo} can be seen on Tab. 1. The difference between the fits and the experiments are described by the relative errors $p_{err} = \mid p_{theo} - p_{fit} \mid / p_{fit}$ and $e_{err} = \mid e_{theo} - e_{fit} \mid / e_{fit}$.

The fits from Eq. 7 on the Fig. 5A and C are in good agreement with the observations. The errors p_{theo} and e_{theo} are relatively low for both experiments. Note that slightly larger errors on p_{theo} and e_{theo} were found for experiments where droplets interact with each other at a larger relative distance r (not showed in this article). From these results, we can say that the Coulomb electric force is adequate to describe the interaction between two electrically charged droplets in this range of droplet charge, radius and speed. In other words, the two electrically charged droplets can be approximated as two point charges in this set of experiments.

In order to highlight the small influence of dipolar forces, more precise measurements are required. This could be achieved by tracking the droplet in the three dimensions. Indeed, during our measurements our principal source of error came from the droplets defocusing from the XZ plan. In particular, the droplet defocus influences the measurement of the constant C from Eq. 7. In order to limit the error on C due to defocus, we chose to measure the constant only on portions where electrically charged droplets were perfectly focused.

Finally, note that a second significant source of error is the accuracy of the microgravity conditions. Indeed, given the droplet radius and charge, an error of 0.05 g is enough to create a force with the same order of magnitude as the electric interaction between two charged droplets spaced of few centimeters. While most of the parabola had a smaller error on the gravity, this g-jitter also explains the difficulty to acquire numerous measurements.

Droplet Impacts

If the electric interaction influences the trajectories of two electrically charged droplets sent toward each other, one can understand that it also influences the impact between electrically charged droplets. In this Section, we focus our attention on experiments where we observed a contact between charged droplets. In the collision diagram for neutral droplets, these experiments correspond to an impact parameter $\chi < 1$. Naturally, the frontier between impact and non-impact between charged droplets can eventually vary. In this Section, we compare the collision diagram for neutral droplets with the collision diagram for charged droplets.

Results

In the case of the collision between neutral drops, both drops moves along a straight line before the impact. Indeed, neutral droplets do not remotely interact with each other. Therefore, the collision parameter $\chi = x/(r_a + r_b)$ is the same whichever the distance r between the droplets. Experimentally, χ is generally calculated when droplets are near each other, in order to minimize any measurement errors. In the case of charged droplets, we showed that the droplet trajectories are influenced by the electric interaction. As a consequence, the distance x in the definition of the collision parameter χ varies over time (see Fig. 1). The main goal of this article is to highlight the possible influence of the electric interaction on the droplet collision. Therefore, the collision parameter was calculated at a particular distance x_i (see Fig. 1) at which the electric force starts to be non-negligible. During the analysis of the impacts between two charged droplets, the electrical force F_{el} (Eq. 3) was considered non-negligible when it corresponded to 15 percent of its maximal value. The limit was chosen in order to minimize the error on the measurements and maximize the influence of the electric force. At this limit, in the range of kinetic energy explored, both droplets are sufficiently far from each other to behave as if they were neutral. Ultimately, note that in further experiments involving better quality of microgravity condition or in simulations, this limit should be reduced toward 0%.

This modification in the calculation of the parameter χ implies that the collision diagram now takes into account the droplet trajectory just before the impact between droplets. In doing this, we highlight any influence of the electric charge just before the impact or during the impact without changing the definition of χ for neutral droplets.

In the case of the parameter We, only a small adjustment on the droplet radius has to be made. Because of the complexity to generate electrically charged droplets in microgravity, the droplet radius may vary from 1 to 15 percent between both interacting droplets. Therefore, each Weber number was associated to an error bar corresponding to the standard deviation calculated from both radii.

In Fig. 2, the red symbols correspond to impacts between charged droplets observed in microgravity. The parameters χ and We were calculated as described in the previous paragraph. The data in Fig. 2 are given with an error bar corresponding to the variation in radii between both droplets. During our experiments, we observed collisions between electrically charged droplets within a wide range of radii and charges ($0.41 < r < 0.97$ mm and $57 < |q| < 190$ pC). According to the Weber number, we observed reflexive collisions (red triangles), stretching separations (red circles) or no collisions at all (red crosses). Collisions between droplets with the same sign of charges are represented by empty circles/triangles while the collision between droplets with opposite sign of charges are represented by full circles/triangles. In order to compare the measurements performed on charged droplets to the collision between neutral droplets, we reported in Fig. 2 the frontier between the different kinds of neutral collisions.

In the case of oppositely charged droplets, because of the difficulty to generate collisions between droplets during parabolic flights, we only observed stretching collisions during our measurements. The majority of these collisions is found in the expected zone of the neutral collision diagram. In other words, we observed mainly no differences between neutral droplet impacts and charged droplet impacts. However, at high collision parameter χ, we observed one reflexive collision in the neutral bouncing region. Even if more observations are needed to draw conclusions, it seems that the reflexive collision region is extended in the case of charged droplets. The observation indicates that the bouncing between two electrically charged droplets with opposite charges could be impossible.

In the same way, the majority of the experiments performed with colliding droplets of the same sign of charge are well located in the neutral collision diagram. However, one specific observation, described as the red cross in Fig. 2, indicates once again that the presence of electric charges affects the boundary of the neutral collision diagram. In this particular case, we observed repulsion between both charged droplets that is sufficient to avoid an impact between them. This observation indicates that repulsion between droplets may be important enough to avoid the collision between droplets in parts of the diagram where $\chi < 1$.

Discussion

We observed two specific experiments where the result of the impact was different from the neutral predictions. Firstly, we observed a stretching separation in the neutral bouncing zone. However, the absence of numerous measurements in the present set of experiment does not allow developing a predictive theory on the whole zone corresponding to droplet bouncing. Indeed, the modeling of the bouncing between two colliding droplets is a difficult problem that was raised several times. Such a phenomenon is linked to several parameters such as the ambient air pressure (Qian and Law 1997), the droplet surface tension or the droplet viscosity. The observation tends to show that the influence of the electric charge of the two droplets can be added to these other variables. Given the last results on the interaction between charged droplets (Bird et al. 2009; Ristenpart et al. 2009), such a behavior is expected. Yet, more quantitative measurements are needed in the case of two droplets impacting each other. In the future, the absence of bouncing between droplets due to their electric interaction could be used for applications in which droplet merging and coalescence is required (e.g. Damak et al. 2016)

Secondly, we observed the non-collision between two charged droplets with the same sign of charge in the part of the diagram corresponding to $\chi < 1$. In the next lines, we suggest a model to answer to this observation. In order to extrapolate the part of the diagram where collisions may be avoided due to the electric repulsion, we investigate the energy conservation in the reference frame corresponding to the center of mass of both droplets.

Thanks to the previous study of charged drop trajectories, we can take the following assumptions: (i) Droplets can be approximated to point charges (which implies a Coulomb interaction); (ii) there is no dissipating force during the droplet motion. By comparing the energy of the system at an infinite distance between droplets to the system energy at the minimum distance between them, we have:

$$\frac{\mu v_{rel}^2}{2} = \frac{k}{r_0} + \frac{\mu C^2}{2r_0^2} \tag{8}$$

The left hand side of the equation corresponds to the kinetic energy of the droplets, with v_{rel} corresponding to the droplet relative speed when they are far from each other. The electric energy is considered equal to zero at an infinite distance. On the right hand side of the equation, the first term corresponds to the electrostatic energy of the system. The distance r_0 corresponds to the minimum distance between droplets. The second term corresponds to the rotational energy of the system. At the minimal distance

between droplets, the kinetic energy of the system equals to zero. Because of the angular momentum definition, we deduce:

$$C = \chi v_{rel}(r_a + r_b) \tag{9}$$

Equation 8 allows to express r_0 as a function of χ. The limit of an impact can be expressed as the point where the distance between the center of mass of the droplet is smaller than the radius of both droplets:

$$r_0 < (r_a + r_b) \tag{10}$$

From Eqs. 8 and 10, we then deduce the following limit for a possible impact between charged droplets:

$$\chi < \sqrt{1 - \frac{V_{e,0}}{E_{k,\text{inf}}}} \tag{11}$$

Where $V_{e,0} = \frac{k}{(r_a+r_b)}$ and $E_{k,\text{inf}} = \frac{\mu v_{rel}^2}{2}$. By knowing $V_{e,0}$ and $E_{k,\text{inf}}$, we can deduce the range of χ for which it is impossible to observe any impact between droplets.

Generally speaking, Eq. 11 indicates that, for charged droplets, the limit of a possible collision is not anymore $\chi = 1$. In the case of two droplets with opposite sign of charges, $\chi > 1$ can lead to collision between droplets. On the other hand, in the case of two droplets with the same sign of charge, collisions can be impossible for $\chi < 1$.

In Fig. 6 (top), the theoretical limitation deduced from Eq. 11 is confirmed by experimental measurements. The droplet speeds v_{rel} were calculated at the same distance where the collision parameter χ were calculated. The green circles correspond to the observation of a non-contact between droplets while the red triangles correspond to the observation of a contact between droplets. The green circle near the orange line (i.e. at the edge between a contact and a non-contact between droplets) corresponds to the red cross presented in Fig. 2. The Fig. 6 (top) not only shows the validity of Eq. 11 but demonstrates also that the Weber number and the collision parameter are not anymore sufficient to completely describe the collision between charged droplets. Indeed, the measurements demonstrate that the electric repulsion/attraction before the impact have to be taken into account.

Therefore, the limit of an impact between charged droplets can only be described on the neutral collision diagram for a given excess of electric charges in both drops. Typically, for a given electric charge, the impact boundary can be plotted as a function of We. Indeed, the Weber number can be introduced in Eq. 11:

$$\chi < \sqrt{1 - \frac{k\rho}{We\mu\gamma}} \tag{12}$$

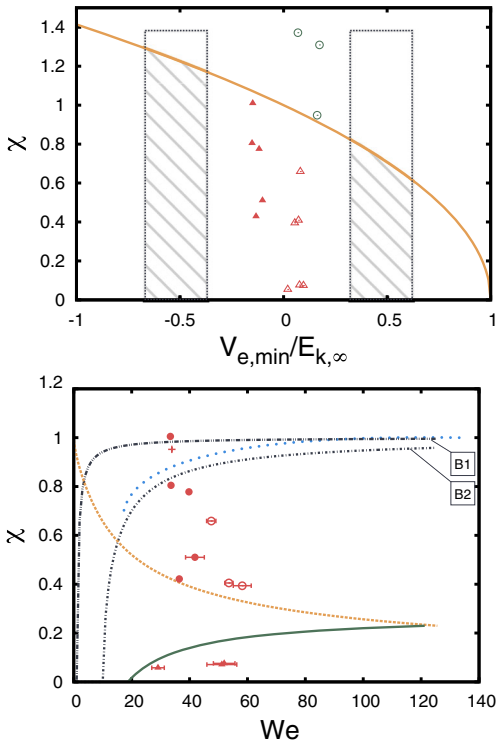

Fig. 6 (Color online) (*top*) Collision parameter χ (Eq. 2) as a function of the ratio between the electric energy and the kinetic energy. The red triangles represent interactions between droplets that lead to an impact. The *green circles* represent interactions between droplets that do not lead to an impact. The orange line corresponds to the limit of a non-impact between droplets (see Eq. 11). (*bottom*) Collision parameter χ as a function of the Weber number We. The *black dash-dotted lines* describe the frontier of an impossible collision in the case of droplets with the same sign of charge. The *lower curve*, named B1, corresponds to the configuration of the experiment described by the red cross in Fig. 2. The *upper curve*, named B2, corresponds to the same experiments but with droplets two times more charged

In the case of the experiment corresponding to the red cross in Fig. 2 (i.e. two droplets with the same sign of charge), the matching frontier is plotted as a black dash-dotted line (B1) in Fig. 6 (bottom). The collisions above the black dash-dotted line are impossible due to charge repulsion. On the contrary, below the black dash-dotted line, the repulsion between droplets is not important enough to avoid collisions.

The frontier shows that, for particular droplet radius and charge, parts of the classic collision diagram are not accessible. Indeed, the Fig. 6 (bottom) shows that a part of the bouncing and the coalescence region is not accessible. Of course, in other configurations, with a more important droplet charge or a smaller radius, a more important part of the neutral collision diagram may be inaccessible. For example, in the case of droplets with a charge two times more important, the second frontier (B2) shows that a larger part of the classic diagram is inaccessible.

Now that a first theory is able to describe the behavior of the collision between charged droplets, the future aim is to confirm the diagrams in Fig. 6 with several measurements on a larger range of energy ratio $V_{e,0}/E_{k,\mathrm{inf}}$. This can be achieved by increasing the droplet charge density or decreasing the droplet relative speed. Still, with these first results, we can already give predictions on the behavior of a diluted gas of charged droplets.

Let us consider a system composed of several charged droplets only interacting with their nearest neighbor. These drops can have different charges and speeds. Therefore, the collision between two droplets is restricted to a certain range of energy ratio $V_{e,0}/E_{k,\mathrm{inf}}$. An example of a range of energy ratio is depicted as the hatched lines in Fig. 6 (top). For this specific range of energy ratio, we can deduce from the Fig. 6 (top) the collision parameter needed for a collision to occur.

If charged droplets collide randomly, the probability of a collision with a specific impact parameter χ_i is uniformly distributed. As a consequence, we observe in Fig. 6 (top) that the collision between droplets with different sign of charges is more likely than the collision between droplets with the same sign of charges. This collision probability is quantified by Eq. 11. Therefore, Eq. 11 could be used to predict the evolution over time of several charged droplets impacting with each other.

Furthermore, the Fig. 11 indicates the limit for which collisions between droplets is impossible for any collision parameter χ. Indeed, if $V_{e,0} = E_{k,\mathrm{inf}}$, impacts between droplets are impossible even for $\chi = 0$. For droplets with a typical charge $q = 50$ pC and radius $r = 1$ mm, this behavior corresponds to a droplet relative speed $v_{rel} = 0.14$ m/s.

Such reasoning on the collision probability between charged droplets can be linked to specific domains of studies. For example, atmospheric research uses a collision efficiency parameter to describe the evolution of a cloud of droplets (charged or not) (Khain et al. 2004; Abbott 1974). Equation 11, which better physically describes the system, could also be used for such a purpose. In other words, Eq. 11 quantifies how likelier to occur is a collision between droplets with opposed charges than between droplets with the same charge. Another domain of interest concerns the spreading of pesticides. Indeed, since several years (Law 2001), farmers use charged droplets to increase the efficiency of the pesticide interaction with plants. New research have also shown that the use of electrically charged droplets could especially increase the spreading of pesticides on hydrophobic surfaces (Damak et al. 2016). In this last case, the collision between charged droplets is primordial. Therefore, Eq. 11 could be used to optimize the collision rate between charged droplets by controlling the energy ratio $V_{e,0}/E_{k,\mathrm{inf}}$ of the system.

Conclusion

In the present work, we were able to study the trajectories of two electrically charged droplets facing each other. The microgravity conditions allowed us to measure the influence of electric charges on the droplets motion, contrary to previous studies (Adam et al. 1968). The results show that taking into account the Coulomb interaction between punctual charges is sufficient to describe the droplet trajectories in the range of droplet speed, charge and radius that were investigated.

Furthermore, when both droplets collide, the result of the collision is influenced by their charges. Contrary to neutral droplet collision, the impact parameter $\chi = 1$ does not define the frontier between collision and non-collision for charged droplets. We were able to determine the limit for a collision to happen as a function of the electric and kinetic energies of the system (see Eq. 11). In particular, we showed that regions of the collision diagram are inaccessible because of the repulsion between droplets with the same sign of charge. Moreover, by predicting the collision probability, Eq. 11 is found useful to describe the evolution over time of a diluted gas of charged droplets. These first experimental and theoretical results lay the foundations for extensive studies on the collision diagram between charged droplets.

Acknowledgments S. D. acknowledges support as a FNRS Senior Research Associate. M. B. acknowledges support as a FNRS-FRIA Fellow. This work has been financed by the project eDroplets funded by Fonds Spéciaux pour la Recherche (FWB) and by ULG ARC Supercool contract. This research has been also funded by the IAP 7/38 MicroMAST initiated by the Belgian Science Policy Office (BELSPO). The authors would also like to warmly thank B. Darbois-Texier, A. Duchesne, J. Hardouin, Bernard Boigelot, M. Mélard, F. Allegro, and S. Rondia for fruitful discussions and development of the experimental setup. We also want to thanks Novespace for all their help through the development of the experiment and during the study itself.

References

Abbott, C.E.: Charged droplet Collision Efficiency Measurements. J. Appl. Meteor **14**, 87 (1974)

Adam, J.R., Lindblad, N.R., Hendricks, C.D.: The collision, coalescence, and disruption of water droplets. J. Appl. Phys. **39**, 5173 (1968)

Ashgriz, N., Poo, J.Y.: Coalescence and separation in binary collisions of liquid drops. J. Fluid Mech. **221**, 183 (1990)

Beard, K.V., Ochs, H.T., Liu, S.: Collision between small precipitation drops. Part III: Laboratory Measurements at Reduced Pressure, vol. 58, pp. 13995. AMS, (2001)

Beard, K.V., Durkee, R.I., Ochs, H.T.: Coalescence Efficiency Measurements for Minimally Charged Cloud Drops. JAS **59**, 233 (2002)

Bird, J.C., Ristenpart, W.D., Belmonte, A., Stone, H.A.: Critical angle for electrically driven coalescence of two conical droplets. PRL **103**, 164502 (2009)

Brandenbourger, M., Dorbolo, S.: Electrically charged droplet: case study of a simple generator. J. Can. Phys. **92**, 1203 (2014)

Brazier-Smith, P.R., Jennings, S.G., Latham, J.: The interaction of Falling Water Drops: Coalescence. Proc. R. Soc. Lond. A **326**, 393 (1972)

Damak, M., Mahmoudi, S.R., Hyder, M.N., Varanasi, K.K.: Enhancing droplet deposition through in-situ precipitation. Nat. Commun. **7**, 12560 (2016)

Davis, M.H., Sartor, J.D.: Theoretical Collision Efficiencies for Small Cloud Droplets in Stokes Flow. Nature **215**, 1371 (1967)

Franklin, C.N., Vaillancourt, P.A., Yau, M.K., Bartello, P.: Collision Rates of Cloud Droplets in Turbulent Flow. AMS **62**, 2451 (2005)

Gotaas, C., Havelka, P., Jakobsen, H.A., Svendsen, H.F.: Evaluation of the impact parameter in droplet-droplet collision experiments by the aliasing method. Phys. Fluids **19**, 102105 (2007)

Imamura, O., Kubo, Y., Osaka, J., Sato, J., Tsue, M., Kono, M.: Observation of sooting behavior in single droplets combustion in direct current electric fields under microgravity. Microgravity Sci. Technol. **17**, 13 (2005)

Khain, A., Arkhipov, V., And, M.: Pinsky rain enhancement and fog elimination by seeding with charged droplets. Part I: Theory and Numerical Simulations. AMS **43**, 1513 (2004)

Law, S.E.: Agricultural electrostatic spray application: a review of significant research and development during the 20th century. J. Electrost. **52**, 25 (2001)

Leblanc, F., Aplin, K.L., Yair, Y., Harrison, R.G., Lebreton, J.P., Blanc, M.: Planetary atmospheric electricity. Space Sci. Rev. **137**, 1 (2008)

Pfeifer, R.J., Hendricks, C.D.: Parametric Studies of Electrohydrodynamic Spraying, vol. 66. AIAA, (1967). Conference paper

Qian, J., Law, C.K.: Regimes of coalescence and separation in droplet collision. J. Fluid Mech. **331**, 59 (1997)

Ristenpart, W.D., Bird, J.C., Belmonte, A., Dollar, F., Stone, H.A.: Non-coalescence of oppositely charged drops. Nature **461**, 377 (2009)

Snarski, S.R., Dunn, P.: Experiments characterizing the interaction between two sprays of electrically charged liquid droplets. Exp. Fluids **11**, 268 (1991)

Swinbank, W.C.: Collisions of Cloud droplets. Nature (London) **159**, 850 (1947)

Testik, F.Y.: Outcome regimes of binary raindrop collisions. Atmos. Res. **94**, 389 (2009)

Visser, C.W., Kamperman, T., Lohse, D., Karperien, M.: APS-DFD. abstract H25.004 (2016)